ACS Sustainable Chemistry & Engineering

Research Article

pubs.acs.org/journal/ascecg

Increasing Desalination by Mitigating Anolyte pH Imbalance Using Catholyte Effluent Addition in a Multi-Anode Bench Scale Microbial Desalination Cell

Robert J. Davis, Younggy Kim,[†] and Bruce E. Logan*

Department of Civil and Environmental Engineering, The Pennsylvania State University, 231Q Sackett Building, University Park, Pennsylvania 16802, United States

Supporting Information

ABSTRACT: A microbial desalination cell (MDC) uses exoelectrogenic bacteria to oxidize organic matter while desalinating water. Protons produced from the oxidation of organics at the anode result in anolyte acidification and reduce performance. A new method was used here to mitigate anolyte acidification based on adding non-buffered saline catholyte effluent from a previous cycle to the anolyte at the beginning of the next cycle. This method was tested using a larger-scale MDC (267 mL) containing four anode brushes and a three cell pair membrane stack. With an anolyte salt concentration increased by an equivalent of 75 mM NaCl using the catholyte effluent, salinity was reduced by 26.0 ± 0.5% (35 g/L NaCl initial solution) in a 10 h cycle, compared to 18.1 ± 2.0% without catholyte addition. This improvement was primarily due to the increase in buffering capacity of the anolyte, although increased conductivity slightly improved performance as well. There was some substrate loss from the anolyte by diffusion into the membrane stack, but this was decreased from 11% to 2.6% by increasing the anolyte conductivity (7.6 to 14 mS/cm). These results demonstrated that catholyte effluent can be utilized as a useful product for mitigating anolyte acidification and improving MDC performance.

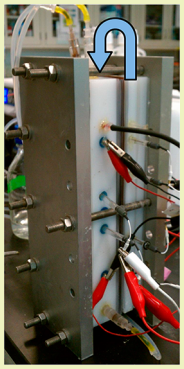

KEYWORDS: *Microbial desalination cell, Desalination, Multi-anode, Anolyte acidification, Electrolyte recycle, MDC*

INTRODUCTION

It is estimated that more than 4 billion people currently live in high water stressed regions in the world, and that 2.5 billion lack safe sanitary practices.[1,2] Conservation and infrastructure improvement can help alleviate some of the water stress, but with the global water shortage projected to grow through 2050 due to the effects of climate change, industrialization, and population growth, new sources of water will be needed.[3] The number of seawater desalination facilities is predicted to increase exponentially in the next 10 years, but current commercial desalination techniques such as electrodialysis, thermal desalination, and reverse osmosis have many environmental concerns and high energy costs.[4,5] Even with state of the art advances in reverse osmosis technology bringing its energy consumption close to the practical theoretical minimum, the energy cost for seawater desalination is still too high for widespread implementation, especially in poorer regions, which are the majority of the water stressed demographic.[6]

A new desalination technology has recently been developed, called a microbial desalination cell (MDC), that uses exoelectrogenic microorganisms to degrade organic matter in wastewater and generate electricity.[7] This process is coupled with a stack of ion exchange membranes to desalinate water and produce energy. One of the main factors limiting MDC performance has been anolyte acidification. As organic matter in wastewater is oxidized by exoelectrogenic bacteria on the anode and electrons are transferred to the electrode, protons are released into solution, lowering the anolyte pH. The rate of proton production at the anode is greater than the rate of buffer diffusion into the anode biofilm, which results in a pH gradient between the solution and biofilm. This creates an acidic environment for the anodic microbial community that can occur even before it is detected in bulk solution.[8] A decrease in the pH below neutral inhibits the respiration of anodic bacteria.[9,10] This pH change is heightened in MDCs as transport of protons from the anode chamber is limited due to the anion exchange membrane in the membrane stack located adjacent to the anode chamber. Similarly, at the cathode, the pH increases when a cation exchange membrane is placed next to the cathode chamber.

Several different approaches have been used to avoid decreases in anode pH such as using larger volumes of electrolyte solutions,[7,11] applying electrolyte recirculation between the cathode and anode chambers,[12,13] or inserting a bipolar membrane next to the anode chamber.[14] Larger electrolyte solution volumes increase cycle time by providing more solution to balance pH, but they require higher operational and capital costs associated with pumping and storing larger volumes of water and do not solve the inherent pH problem. Electrolyte recirculation extends cycle time by balancing protons accumulated in the anode chamber with hydroxide ions that are formed in the cathode chamber, but the

Received: May 17, 2013
Revised: June 24, 2013
Published: June 28, 2013

introduction of organic matter into the cathode chamber can result in extensive biofouling of the cathode and low Coulombic efficiencies (<25%). A bipolar membrane can be used instead of the anion exchange membrane next to the anode chamber to dissociate water and balance pH. However, a large voltage (1.0 V) must be used due to the high resistance of the bipolar membrane, which makes the process energy intensive.

A different approach was used here to mitigate anolyte pH imbalance based on using the cathode solution. Instead of recycling electrolyte solutions between the electrode chambers, the non-buffered and saline catholyte effluent was mixed once with fresh anolyte to increase the anolyte alkalinity and ionic conductivity. Oxygen reduction reaction at the cathode consumes protons and increases the pH to approximately 12.8. The catholyte has a high conductivity due to the salinity of the water being desalinated (~70 mS/cm with 35 g/L NaCl). Therefore, adding the catholyte to the anolyte increases the conductivity of the anolyte solution and reduces internal resistance. The effectiveness of amending the anolyte with catholyte was examined here using a larger-scale multi-anode electrode MDC in terms of current production, desalination, power generation, and COD removal. The transport of anions out of the anode chamber during a cycle by back-diffusion was also measured to determine substrate losses from the anode chamber. Additional experiments were conducted by adding NaCl directly to the anolyte, allowing observation of the effect of conductivity separately from that produced by catholyte pH.

MATERIALS AND METHODS

MDC Construction. The anode and cathode chambers were constructed using high density polyethylene (HDPE) material with a cross-sectional area of 52.5 cm^2 (17.5 cm × 3 cm) (Figure 1). The

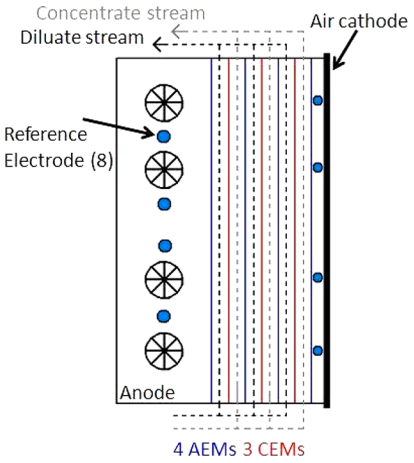

Figure 1. Schematic of bench scale MDC with parallel continuously recycled flow through the three cell pair electrodialysis stack. AEM: anion exchange membrane. CEM: cation exchange membrane.

anode chamber had a volume of 160 mL, and the cathode chamber had a volume of 53 mL to minimize the distance between electrodes. Four bars of HDPE (0.5 cm height) were evenly spaced and placed on the inner face of both chambers in order to prevent membrane deformation. Four heat-treated graphite fiber brushes 2.7 cm in diameter and 2.3 cm long were used as the anodes (Mill-Rose Lab Inc., U.S.A.).[15] The air cathodes consisted of wet-proofed carbon cloth (30%), with four layers of polytetrafluoroethylene diffusion layers, a Nafion binder, and 0.5 mg Pt/cm^2.[16] The anodes were each connected to individual 10 Ω external resistors and connected in parallel to the cathode through a single titanium wire current collector along the length of the cathode.

The electrodialysis stack consisted of three cell pairs made of interchanging anion and cation exchange membranes (Selemion CMV and AMV, Asahi glass, Japan) pretreated in a 0.6 M NaCl solution for 24 h and then rinsed with deionized water. The silicone gaskets used to make a water tight seal in the stack had a thickness of 1.3 mm, and polyethylene mesh spacers (2.5 cm × 16 cm) were used to maintain cell thickness. Each cell held approximately 9 mL. The gaskets and membranes were cut to allow parallel flow through the stack, entering and leaving through the anode side of the reactor. Ag/AgCl reference electrodes (RE-5B; BASi, West Lafayette, IN) were placed between the anodes in the anode chamber and directly across from the anodes in the cathode chamber. The reactor was bolted together using anodized aluminum plates on each side of the reactor.

Medium. The anodes were inoculated (50% v/v) with a preacclimated mixed culture community of microorganisms from a functioning acetate-fed MFC and acclimated individually in 4 cm cube reactors with a 10 Ω external resistor for over one month. NaCl concentrations were gradually increased from 0 to 200 mM NaCl in order to preacclimate bacteria to higher Cl^- conditions typically produced in the MDC.[17] The anode chamber of the MDC was fed a solution of sodium acetate (1 g/L) in a 50 mM phosphate buffer solution containing (per liter of deionized water): 0.31g NH_4Cl, 2.45g $NaH_2PO_4{\cdot}H_2O$, 4.58g Na_2HPO_4, 0.13g KCl, 5 mL vitamins, and 6.25 mL trace minerals.[18] The catholyte, diluate, and concentrate solutions were all synthetic seawater consisting of 35 g/L NaCl prepared in deionized water.

MDC Operation and Experimental Procedures. The cathode chamber was operated in fed-batch mode. The solution in the anode chamber was continuously recycled at 1.0 mL/min (from the bottom to the top of the chamber) to avoid localized differences in substrate concentrations that could affect reactor performance.[19] The reactor was left in open circuit for an hour previous to operation, with 35 g/L NaCl solution flushed through the stack at 5 mL/min to remove solution from the previous cycle. During operation, the diluate solution was continuously recycled using a 100 mL reservoir. The concentrate stream was continuously recycled to a larger reservoir (~450 mL) to minimize the salinity increase in this chamber. Both streams had a flow rate of 1 mL/min. The cycle time was set to 10 h to minimize osmotic losses at the end of a cycle when current decreased to lower levels.

Catholyte effluent (~70 mS/cm, pH ~12.8) collected from a previous cycle was added to the anolyte influent, rather than using the catholyte from the same cycle, to simplify MDC operation. The volume of catholyte used was evaluated in terms of the equivalent change in salt concentration, producing increments of 25, 50, and 75 mM higher anolyte salt concentrations. The substrate concentration was maintained at 1 g/L acetate to avoid the effects of the different initial substrate concentrations on performance. The amount of PBS added to the anolyte was also constant for each experimental condition (Figure S1, Supporting Information). At 100 mM PBS, current was produced with a maximum salt concentration addition from catholyte of 150 mM. Therefore, with 50 mM PBS as the anolyte, the highest salt concentration from catholyte addition used was 75 mM. As a control, a fed-batch cycle was run without addition of catholyte effluent to the anolyte solution. Addition of catholyte effluent increased both conductivity and pH of the anolyte. In order to observe the effect of conductivity separately from pH, in separate experiments, sodium chloride was added to the anolyte at 25, 50, and 75 mM NaCl increments, avoiding a pH change.

Analyses and Calculations. The voltage (U) for each anode across a 10 Ω external resistor[11] was measured at 10 min intervals using a multimeter (Keithley Instruments, U.S.A.) connected to a personal computer. Current was calculated as $i = U/R$, and current density was normalized by the cathode surface area (52.5 cm^2). Influent and effluent solutions for diluate, concentrate, anolyte and catholyte solutions were analyzed using conductivity and pH probes (SevenMulti, Mettler-Toledo International, Inc., U.S.A.). The total desalination rate (g/L−d) was calculated as the change in salinity

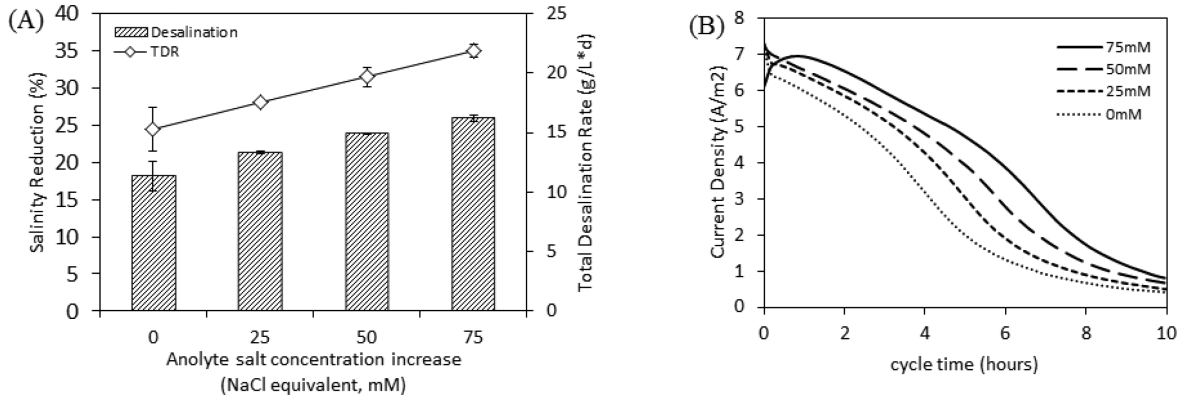

Figure 2. (A) Extent of desalination and total desalination rate with increasing anolyte salt concentration increase from catholyte effluent addition. (B) Current density profile during one 10 h cycle for different amounts of catholyte effluent addition.

based on total dissolved solids. The salinity was estimated from conductivity measurements using an in situ conductivity conversion as previously outlined by Bennett[20] and assuming the conductivity measured was due only to NaCl. Current efficiency (η) was determined as ratio of ionic separation of NaCl to the total number of electrons passed through the circuit, as

$$\eta = \frac{F(c_{in}^{D}v_{in}^{D} - c_{out}^{D}v_{out}^{D})}{N_{cp}\sum \int i dt} \quad (1)$$

where F is Faraday's constant, c the molar concentration of NaCl in the diluate, v the volume of the diluate, N_{cp} the number of cell pairs in the electrodialysis stack, and i the current generated in the reactor. The subscript "in" indicates conditions at the beginning of the cycle, "out" the end of the cycle, and the superscript "D" indicates diluate.[17]

The chemical oxygen demand (COD) was measured for influent and effluent anolyte solutions using standard methods (Hach Co., U.S.A.). The COD sample was diluted at a 1:10 ratio in order to minimize the effect of chloride ions on measurements. The Coulombic efficiency (CE) was calculated based on the total COD removed and the number of coulombs collected during the cycle as previously described.[21] The Coulombic efficiency calculated here was modified to account for acetate losses due to diffusion out of the anode chamber, as

$$CE_{diff} = \frac{M_{O2}\int_0^t I dt}{F b_{es} v_{an}(COD_{in} - COD_{eff} + COD_{diff})} \quad (2)$$

where M_{O2} is the molecular weight of O_2 (32 g/mol), b_{es} the number of electrons exchanged per mole of oxygen (4 mol e^-/mol O_2), COD_{in} the measured substrate concentration at the beginning of the cycle, COD_{eff} the measured concentration at the end of the cycle, and COD_{diff} the substrate concentration measured in the adjacent diluate solution due to diffusion through the membrane.

Diluate samples were analyzed for phosphate using ion chromatography (IC, Dionex ICS-1100) and acetate using high performance liquid chromatography (HPLC, Shimadzu LC-20AT). The power density was measured for each experimental condition using an external resistance ranging from 10 to 10,000 Ω at 20 min intervals, after the reactor was initially set at open circuit for ~1 h. During polarization tests, salt solution (35 g/L NaCl) was continuously flowed through the electrodialysis stack at a flow rate of 5 mL/min in order to minimize losses due to junction potential and to decrease internal resistance as previously demonstrated.[17] Power densities (mW/m^2) were normalized by the cathode projected surface area.

RESULTS

Desalination and Current Generation. The MDC was run under four different operating conditions, each with varying amounts of catholyte effluent added to the anolyte. The salt concentration in the diluate solution (35 g/L NaCl) was reduced by 26.0 ± 0.5% when the anolyte salt concentration was increased by 75 mM using the catholyte effluent, compared to 18.1 ± 2.0% in the control (no catholyte addition). The total rate of desalination and extent of desalination increased linearly with catholyte concentration because the cycle time was fixed (Figure 2a). The peak current density was 7.21 ± 0.08 A/m^2 shortly after the circuit was closed for two lowest catholyte additions (25 and 50 mM) and the control. For tests with 75 mM catholyte, the current density was initially lower at 6.10 A/m^2, but it increased to a maximum of 6.95 A/m^2 after 40−60 min (Figure 2b). The number of coulombs recovered increased with catholyte addition from 532 C (no catholyte) to 833 C (75 mM catholyte). Diluate recovery averaged 90%, with a anolyte:diluate effluent ratio of 1.4:1. Fouling was not observed on the cathode.

The maximum power density was 685 mW/m^2 with either 50 or 75 mM catholyte addition (Figure 3). When the anolyte

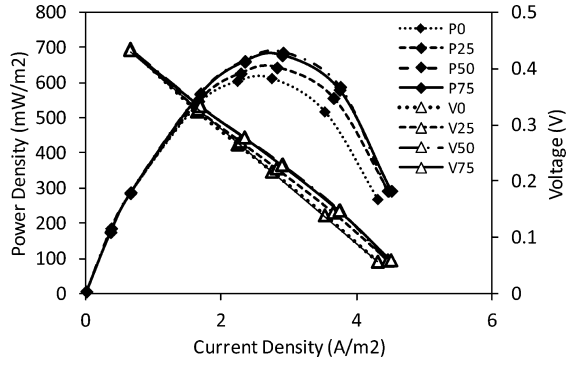

Figure 3. Maximum power density with various amounts of catholyte effluent addition (0−75 mM) after ~30 days of operation at 10 Ω external resistance. The internal resistance is also shown by the slope of the voltage with respect to current. The closed diamonds "P" represent power density at a given concentration of catholyte addition, while the open signs "V" are for voltage.

conductivity was nearly doubled from 7.6 ± 0.1 to 14.3 ± 0.9 mS/cm through addition of the 75 mM equivalent catholyte, the total internal resistance decreased by only 5 to 73 Ω (based on the slopes of the polarization data). This suggests that the anolyte solution resistance was not a large fraction of the overall internal resistance. The average power production over the fed-batch cycle was 318 ± 14 mW/m^2 with the 75 mM catholyte

addition, and this power density decreased linearly with smaller volumes of catholyte addition (Figure S2, Supporting Information). The external resistance of the MDC was set to maximize current and therefore desalination rate rather than power production. Increasing the external resistance could yield higher power densities as discussed by Jacobson et al.[22]

The catholyte effluent pH was 12.8 ± 0.3, so amending fresh anolyte solution with catholyte effluent resulted in a higher initial anolyte pH. The initial anolyte pH was 8.12 ± 0.40 with 75 mM catholyte addition. The initial pH approached a more neutral pH with smaller volumes of catholyte addition, with a pH of 7.17 ± 0.03 for the control (no catholyte addition) (Figure 4). Greater volumes of catholyte effluent addition

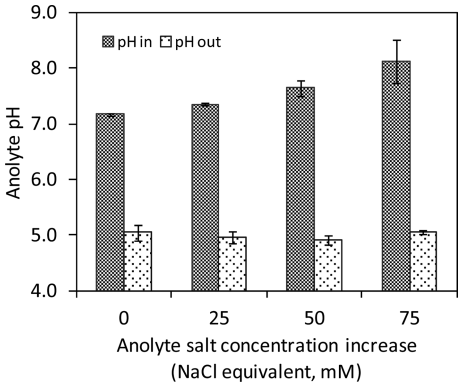

Figure 4. Anolyte pH at the beginning and end of one cycle at various concentrations of anolyte salt increases due to catholyte effluent addition. Increasing the amount of catholyte effluent addition results in an increase of initial anolyte pH.

increased the extent of desalination (Figure 2a) but too high an initial pH limited microbial current generation. In separate tests with greater amounts of catholyte addition than those reported here, it was observed that an initial anolyte pH above 9.0 irreversibly decreased current generation to zero (Figure S3, Supporting Information), as also shown by others.[23] The improvement in desalination performance is attributed to the increase in anolyte pH from catholyte addition rather than the increase in anolyte conductivity, as adding 75 mM NaCl to the anolyte resulted in a 2% drop in desalination. The pH at the end of the cycle was 5.0 ± 0.1 under all experimental conditions, which is in the low pH range known to inhibit current generation.[9]

Anion Transport and Effect on COD Removal. The current efficiency is the fractional contribution of the total electrons transferred through the circuit for ionic separation in the dilute solution. The average current efficiency here was 96 ± 7% (eq 1), demonstrating that the ion exchange membranes effectively transported sodium or chloride counterions with current generation and little back-diffusion of these ions. Other counterions could back-diffuse across the ion exchange membranes, although this is not accounted for in eq 1. There was back-diffusion of acetate and phosphate anions across the anion exchange membrane into the adjacent diluate chamber. This diffusion resulted in a loss of 0.03 ± 0.02 g/L of acetate from the anode chamber with 75 mM catholyte addition, and this increased to as much as 0.11 ± 0.02 g/L with no catholyte addition (control). Phosphate ions were also lost from the anode chamber, increasing from 2.3 mM PO_4^{3-} (75 mM catholyte addition, 14.3 mS/cm) to 3.2 mM PO_4^{3-} (control, 7.6 mS/cm) (Figure 5a). This trend of decreasing diffusive anion transport was also apparent when NaCl (not catholyte) was directly added to the anolyte, demonstrating that anion back-diffusion out of the anode chamber was a function of anolyte conductivity.

Final acetate concentrations in the anode chamber decreased with higher concentrations of catholyte added to the anolyte, with acetate removals ranging from 55.2 ± 1.7% (control) to 62.8 ± 0.4% (75 mM catholyte addition). The greater COD removal was due to higher current densities associated with catholyte addition. When increasing anolyte conductivity using only NaCl, there was less COD removal (Figure 5b), which indicated that it was the additional buffering capacity due to the catholyte rather than the increased conductivity that improved the extent of substrate oxidation. COD removal from biochemical processes was less than that measured in the anode chamber due to acetate diffusion through the adjacent ion exchange membrane. The effect of diffusion on correcting microbial COD removal was greatest at lower conductivity anode solutions, decreasing COD removal by 17% compared to the control (7.6 mS/cm) (Figure 6).

The CE ranged from 59% to 87%, indicating that very little oxygen diffused to the anode biofilm. CE increased with greater amounts of catholyte effluent addition, from 59 ± 3% (control),

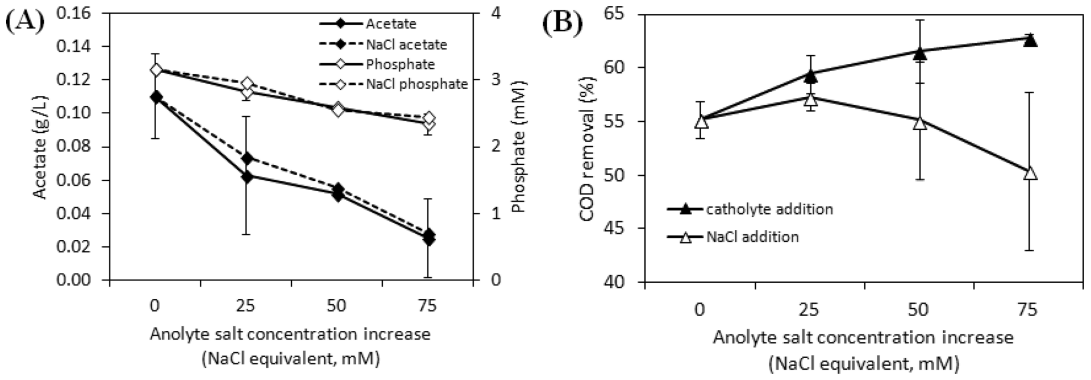

Figure 5. (A) Diffusion of acetate and phosphate,PO_4^{3-} across the anion exchange membrane from the anolyte chamber into the diluate solution. The dashed line denotes experiments with NaCl added to the anolyte, while the solid lines are data from experiments with catholyte addition. (B) COD removal at various increments of NaCl addition with no effect on anolyte pH (open signs) and due to addition of catholyte effluent with an increase in anolyte pH (closed signs). Results are displayed at various increments of anolyte salt concentration increase due to either NaCl addition or catholyte effluent addition.

dx.doi.org/10.1021/sc400148j | ACS Sustainable Chem. Eng. 2013, 1, 1200−1206

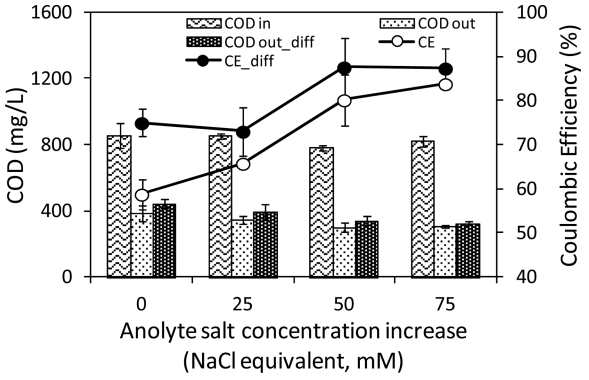

Figure 6. Coulombic efficiencies and COD measurements from the anolyte at the beginning and end of one cycle for various increments of anolyte salt concentration increase due to catholyte effluent addition. The subscript "diff" indicates data points where diffusion of acetate out of the anode chamber was taken into account.

66 ± 1% (25 mM catholyte), 80 ± 6% (50 mM catholyte), to 84 ± 1% (75 mM catholyte). The changes in the CE_{diff} were less variable when acetate losses due to diffusion were included, ranging from 75 ± 3% (control) to 87 ± 4% (75 mM). The effect of acetate diffusion on CE_{diff} was greatest at lower anolyte conductivities (28% increase at 7.6 mS/cm) and lessened with higher anolyte conductivity (4% increase at 14.3 mS/cm) (Figure 6).

Effect of Anolyte Recirculation on Anode Performance. Anolyte recirculation resulted in a more equal distribution of current generation along the height of the reactor and improved overall current density. When the anode chamber was initially filled (batch mode), each anode contributed almost equally to performance based on measured currents. The nearly equal current production by each anode at the beginning of the cycle indicates that when the anode chamber was initially filled, it functioned as a completely mixed reactor. As the cycle progressed, however, the current produced by the anode at the top of the reactor first declined, followed successively by the other anodes down along the length of the reactor (Figure 7b). The difference in current generation from each anode was most likely caused by a substrate gradient that developed over time as has been observed by others.[24,25] Over eight 24 h fed-batch cycles, the contribution of the top anode toward current generation decreased from 37% to 11% suggesting that there were differences in substrate concentrations developing within the reactor over time.

To test the hypothesis that substrate gradients within the anode chamber were producing different current production by the anodes, the anolyte was recycled from the bottom to the top of the reactor at 1 mL/min. Anolyte recirculation successfully balanced the contribution of current from each anode (Figure 7a) and increased total current generation by 7.9 ± 2.2% based on total coulombs recovered in the circuit. The COD removal increased to 86 ± 4% (recycle) from 78 ± 3% (batch). Recirculation minimized the difference in anode potentials between electrodes and had a minimal effect on cathode potentials (Figure S4, Supporting Information).

DISCUSSION

Catholyte effluent addition increased desalination and substrate removal in the MDC by delaying anode acidification, although a near neutral anolyte pH was not sustained for the full cycle. Fed-batch addition of catholyte to the anolyte at the beginning of the cycle was only partly successful in improving anode performance, as the initial current density was slightly inhibited with 75 mM addition (6.10 A/m^2) compared to the control (7.21 A/m^2) due to a higher initial pH. Adding too much catholyte at the beginning of the cycle also detached the biofilm. In future tests, an incremental addition of catholyte could be used to better mitigate anolyte acidification throughout the whole cycle. This addition of catholyte over the whole cycle would avoid a high initial pH, allowing for a greater total catholyte volume to be used. For incremental addition to be effective, the catholyte must have a high pH at an early stage of the cycle. This could be done by using a large cathode surface area to volume ratio. Performance would not improve indefinitely with greater catholyte addition, as Cl^- ions from the adjacent diluate stream, with the addition of high concentrations of NaCl from the catholyte, could also inhibit microbial activity.

COD removal and number of recovered coulombs increased with catholyte effluent addition, but the approach used here did not take into account substrate dilution resulting from catholyte addition. The initial substrate concentration (1 g/L sodium acetate) was kept constant in order to minimize the number of variables in the system during experiments. The addition of catholyte would have decreased the substrate concentration by 6% (25 mM), 10% (50 mM), and 15% (75 mM catholyte addition). Small changes in the initial concentrations of COD

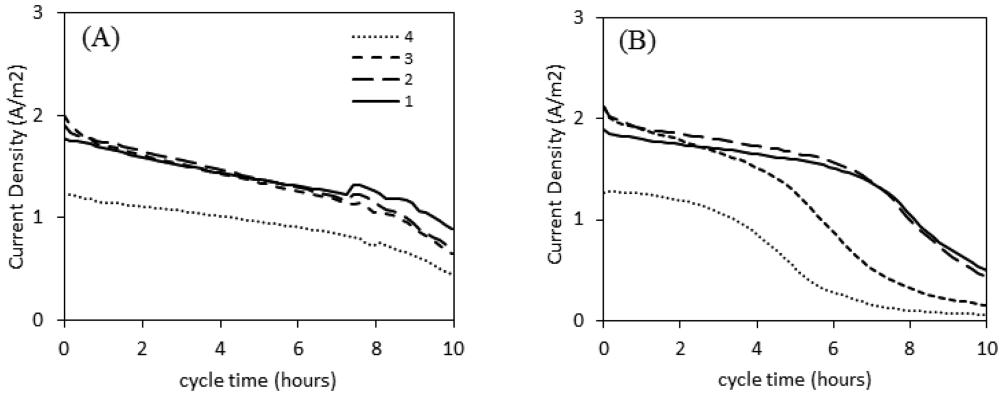

Figure 7. (A) Current density contribution from each anode with anolyte recycle and (B) in fed-batch mode. The electrodes are ordered from the bottom (1) to the top anode (4).

(>850 mg COD/L) would have had little effect on power generation, but at lower COD concentrations power can decrease substantially with the COD concentration.[24,26,27] Substrate concentration is therefore only a factor at lower COD concentrations. At high COD concentrations, other factors are more important for maximizing current production such as pH and conductivity. Substrate dilution could therefore have an impact on performance of the MDC with either incremental or continuous addition of the catholyte to anolyte, in terms of reduced cycle times, desalination rates, or extent of desalination.

Substrate losses by anion diffusion out of the anode chamber affected both the CE_{diff} and COD removal. The CE is a measure of the ratio of recovered coulombs as current to the total theoretical amount of coulombs that could be produced by the oxidized substrate. Losses in CE typically arise from the use of alternate electron acceptors by the bacteria on the anode, such as oxygen, or from the incomplete oxidation of a substrate. The CE typically is calculated based only on current production, with the assumption that all of the other substrate losses are due to other biological processes.[21] However, as shown in MDC tests here, there was significant loss (11%) of substrate through physical diffusion through the membrane. When an anion exchange membrane is placed adjacent to the anode chamber, transport of negatively charged species, such as acetate anions, should be measured and accounted for in the COD removal and CE calculations (eq 2). In a two chamber MFC, substrate losses through the membrane have also been shown to decrease cathode electrode performance.[28] Without considering substrate diffusion, total COD degradation will be overestimated and CE underestimated.

In considering scale up of MDCs, two important factors are the ratio of substrate to diluate volumes and the desalination rate. Many MDCs have been shown to achieve over 90% desalination of saline water, but these extents of desalination have required 13−66 times more anolyte volumes than the volume of desalinated water produced in the process (Figure 8). The use of such large volumes of anolyte solutions is not practical for scale up due to high capital and operational costs. A high level of desalination has also previously required over 48 h.[22,29] A long fed-batch cycle time results in a small rate of desalted water production.[30,31] The desalination rate produced here using the bench scale MDC was 22.5 g/L−d, with an anolyte volume 1.4 times that of the diluate effluent. The only report of a similar desalination rate required the use of 66 times more anolyte to desalination effluent.[7] Design aspects used here that improved performance compared to these previous studies were the rectangular shape of the reactor, which minimized the possibility for dead zones in the stack; use of a larger concentrate solution to decrease osmotic water losses from adjacent cells; use of thin electrodialysis cells to minimize solution resistances; and choosing a more optimal cycle time based on ending the cycle at a time that maximized the extent of desalination, avoiding back diffusion of ions from the concentrate to diluate chambers (Figure S5, Supporting Information). The concentrate solution increased slightly to 37.2 ± 0.1 g/L and could be reused as either fresh catholyte or desalination solution. The diluate volume in this operation was also easily adjustable because diluate was collected in a separate container and recycled through the stack. If a smaller diluate volume had been used, greater desalination would be expected.

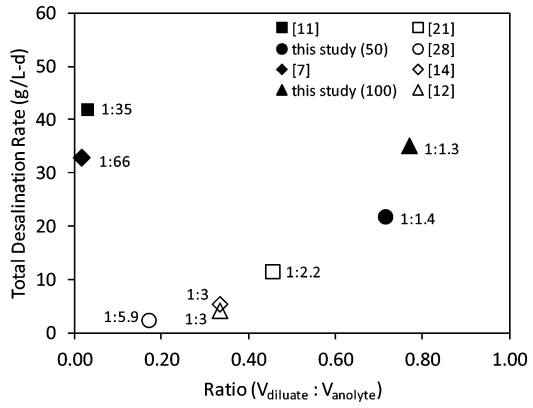

Figure 8. Comparison of diluate solution to anolyte volume ratio and total desalination rate of various studies. The (50) and (100) values for "this study" indicate PBS concentration (mM) of the anolyte. An ideal MDC would be in the upper right-hand corner: high diluate to anolyte ratio and high total desalination rate.

Recycling the anolyte was shown here to have a positive effect on MDC performance. The average current output when the anolyte was recycled was 8% higher than that obtained in batch mode operation (no recycle). While the exact reason for this change is not known, current generation without recycle may have resulted in the development a substrate gradient along the length of the anode chamber during batch mode operation. It was observed that electrodes near the top of the reactor also produced less current than those at the bottom. Recycling anolyte from the bottom to the top would have eliminated the development of substrate gradients in the anode chamber, facilitated better mass transport of substrate to the biofilm, and increased ion transport into and out of the biofilm. Transport of protons from the biofilm into solution can hinder microbial activity on the anode due to the development of localized low pH.[8,10] Pumping fluid through the anode chamber could have reduced concentration boundary layers around the anode and improved ion transport rates and therefore pH gradients in the biofilm. The recycle rate used here was low (1 mL/min), resulting in replacement of about 0.4 times the volume of the anolyte per hour. However, increasing the recycle rate to 2 mL/min decreased current densities over three cycles for reasons which are not known (data not shown). Other studies have reported the use of much higher recycle rates. For example, an upflow MFC recycled 3.5 and 12.5 times the volume of anolyte per hour and reported 38% and 46% improvement in current generation, respectively.[32] The results obtained here suggest that reactor performance can be improved using only minimal recirculation.

■ ASSOCIATED CONTENT

Supporting Information

Additional figures, as referenced in text, describe the composition of the anolyte using the catholyte, average power with different amounts of catholyte, current densities, pH, and solution conductivities. This material is available free of charge via the Internet at http://pubs.acs.org.

■ AUTHOR INFORMATION

Corresponding Author

*E-mail: blogan@psu.edu.

Present Address

[†]Younggy Kim: Department of Civil Engineering, McMaster University, Hamilton, ON L8S 4L7, Canada

Notes

The authors declare no competing financial interest.

■ ACKNOWLEDGMENTS

The authors thank Siemens Corp. for kindly donating an electrodialysis reactor as a design reference for this project, Hiroyuki Kashima for his help with ion chromatography, and Dr. Xiuping Zhu for conducting the HPLC analysis. This research was supported by Award KUS-11-003-13 from the King Abdullah University of Science and Technology (KAUST).

■ REFERENCES

(1) Vorosmarty, C.; McIntyre, P.; Gessner, M.; Dudgeon, D.; Prusevich, A.; Green, P.; Glidden, S.; Bunn, S.; Sullivan, C.; Liermann, C.; Davies, P. Global threats to human water security and river biodiversity. *Nature* **2010**, *467*, 555.

(2) *Progress on Drinking Water and Sanitation*; World Health Organization and UNICEF: Geneva, Switzerland, 2012.

(3) Oki, T.; Kanae, S. Global hydrological cycles and world water resources. *Science* **2006**, *313*, 1068.

(4) Zhou, Y.; Tol, R. Evaluating the costs of desalination and water transport. *Water Resour. Res.* **2005**, *41* (3), 1−10.

(5) Christen, K. Environmental costs of desalination. *Environ. Sci. Technol.* **2007**, *41*, 5579.

(6) Elimelech, M.; Phillip, W. The future of seawater desalination: Energy, technology, and the environment. *Science* **2011**, *333*, 712.

(7) Cao, X.; Huang, X.; Liang, P.; Xiao, K.; Zhou, Y.; Zhang, X.; Logan, B. A new method for water desalination using microbial desalination cells. *Environ. Sci. Technol.* **2009**, *43*, 7148−7152.

(8) Franks, A.; Nevin, K.; Jia, H.; Izallalen, M.; Woodard, T.; Lovely, D. Novel strategy for three-dimensional real-time imaging of microbial fuel cell communities: Monitoring the inhibitory effects of proton accumulation within the anode biofilm. *Energy Environ. Sci.* **2009**, *2*, 113−119.

(9) He, Z.; Huang, Y.; Manohar, A.; Mansfeld, F. Effect of electrolyte pH on the rate of the anodic and cathodic reactions in an air−cathode microbial fuel cell. *Bioelectrochemistry* **2008**, *74*, 78−82.

(10) Torres, C.; Marcus, A.; Rittmann, B. Proton transport inside the biofilm limits electrical current generation by anode-respiring bacteria. *Biotechnol. Bioeng.* **2008**, *100* (5), 872−881.

(11) Chen, X.; Xia, X.; Liang, P.; Cao, X.; Sun, H.; Huang, X. Stacked microbial desalination cells to enhance water desalination efficiency. *Environ. Sci. Technol.* **2011**, *45*, 2465−2470.

(12) Qu, Y.; Feng, Y.; Wang, X.; Liu, J.; Lv, J.; He, W.; Logan, B. Simultaneous water desalination and electricity generation in a microbial desalination cell with electrolyte recirculation for pH control. *Bioresour. Technol.* **2012**, *106*, 89−94.

(13) Chen, X.; Liang, P.; Wei, Z.; Zhang, X.; Huang, X. Sustainable water desalination and electricity generation in a separator coupled stacked microbial desalination cell with buffer free electrolyte circulation. *Bioresour. Technol.* **2012**, *119*, 88−93.

(14) Chen, S.; Liu, G.; Zhang, R.; Qin, B.; Luo, Y. Development of the microbial electrolysis desalination and chemical-production cell for desalination as well as acid and alkali productions. *Environ. Sci. Technol.* **2012**, *46*, 2467−2472.

(15) Logan, B.; Cheng, S.; Watson, V.; Estadt, G. Graphite fiber brush anodes for increased power production in air−cathode microbial fuel cells. *Environ. Sci. Technol.* **2007**, *41*, 3341−3346.

(16) Cheng, S.; Liu, H.; Logan, B. E. Increased performance of single-chamber microbial fuel cells using an improved cathode structure. *Electrochem. Commun.* **2006**, *8*, 489−494.

(17) Kim, Y.; Logan, B. Series assembly of microbial desalination cells containing stacked electrodialysis cells for partial or complete seawater desalination. *Environ. Sci. Technol.* **2011**, *45*, 5840−5845.

(18) Cheng, S.; Xing, D.; Call, D.; Logan, B. Direct biological conversion of electrical current into methane by electromethanogenesis. *Environ. Sci. Technol.* **2009**, *43* (10), 3953−3958.

(19) Ahn, Y.; Logan, B. Domestic wastewater treatment using multi-electrode continuous flow MFCs with a separator electrode assembly design. *Appl. Microbiol. Biotechnol.* **2013**, *97*, 409−416.

(20) Bennett, A. S. Conversion of in situ measurements of conductivity to salinity. *Deep-Sea Res.* **1976**, *23*, 157−165.

(21) Logan, B. *Microbial Fuel Cells*; John Wiley & Sons, Inc.: Hoboken, NJ, 2008.

(22) Jacobson, K.; Drew, D.; He, Z. Use of a liter-scale microbial desalination cell as a platform to study bioelectrochemical desalination with salt solution or artificail seawater. *Environ. Sci. Technol.* **2011**, *45*, 4652−4657.

(23) Patil, S.; Harnisch, F.; Koch, C.; Hubschmann, T.; Fetzer, I.; Carmona-Martinez, A.; Muller, S.; Schroder, U. Electroactive mixed culture derived biofilms in microbial bioelectrochemical systems: The role of pH on biofilm formation, performance and composition. *Bioresour. Technol.* **2011**, *102*, 9683−9690.

(24) You, S.; Zhao, Q.; Zhang, J.; Jiang, J.; Wan, C.; Du, M.; Zhao, S. A graphite-granule membrane-less tubular air-cathode microbial fuel cell for power generation under continuously operational conditions. *J. Power Sources* **2007**, *173*, 172−177.

(25) Karra, U.; Troop, E.; Curtis, M.; Scheible, K.; Tenaglier, C.; Patel, N.; Li, B. Performance of plug flow microbial fuel cell (PF-MFC) and complete mixing microbial fuel cell (CM-MFC) for wastewater treatment and power generation. *Int. J. Hydrogen Energy* **2013**, *38* (13), 5383−5388.

(26) Jiang, D.; Li, B. Granular activated carbon single-chamber microbial fuel cells (GAC-SCMFCs): A design suitable for large-scale wastewater treatment processes. *Biochem. Eng. J.* **2009**, *47*, 31−37.

(27) Cheng, S.; Logan, B. Increasing power generation for scaling up single-chamber air cathode microbial fuel cells. *Bioresour. Technol.* **2011**, *102*, 4468−4473.

(28) Harnisch, F.; Wirth, S.; Schroder, U. Effects of substrate and metabolite crossover on the cathodic oxygen reduction reaction in microbial fuel cells: Platinum vs. iron(II) phthalocyanine based electrodes. *Electrochem. Commun.* **2009**, *11*, 2253−2256.

(29) Luo, H.; Xu, P.; Roane, T.; Jenkins, P.; Ren, Z. Microbial desalination cells for improved performance in wastewater treatment, electricity production, and desalination. *Bioresour. Technol.* **2012**, *105*, 60−66.

(30) Mehanna, M.; Saito, T.; Yan, J.; Hickner, M.; Cao, X.; Huang, X.; Logan, B. Using microbial desalination cells to reduce water salinity prior to reverse osmosis. *Energy Environ. Sci.* **2010**, *3*, 1114−1120.

(31) Kim, Y.; Logan, B. Microbial desalination cells for energy production and desalination. *Desalination* **2013**, *308*, 122−130.

(32) Zhang, F.; Jacobson, K.; Torres, P.; He, Z. Effects of anolyte recirculation rates and catholytes on electricity generation in a litre-scale upflow microbial fuel cell. *Energy Environ. Sci.* **2010**, *3*, 1347−1352.